COLLECTION, PRODUCTION AND STORAGE OF BLOOD COMPONENTS

Original article

Ultraviolet light and riboflavin accelerates red blood cell dysfunction *in vitro* and in a guinea pig transfusion model

Jin Hyen Baek[1*], Hye Kyung H. Shin[1], Fei Xu[2], Xiaoyuan Zhang[1], Matthew C. Williams[1], Yamei Gao[3], Jaroslav G. Vostal[2], Paul W. Buehler[4], Carlos Villa[5], Felice D'Agnillo[1*]

[1]*Laboratory of Biochemistry and Vascular Biology, Division of Blood Components and Devices, Center for Biologics Evaluation and Research, Food and Drug Administration, Silver Spring, MD, United States of America*
[2]*Laboratory of Cellular Hematology, Division of Blood Components and Devices, Center for Biologics Evaluation and Research, Food and Drug Administration, Silver Spring, MD, United States of America*
[3]*Division of Viral Products, Center for Biologics Evaluation and Research, Food and Drug Administration, Silver Spring, MD, United States of America*
[4]*University of Maryland School of Medicine, Center for Blood Oxygen Transport and Hemostasis and the Department of Pathology, Baltimore, MD, United States of America*
[5]*Office of Blood Research and Review, Center for Biologics Evaluation and Research, Food and Drug Administration, Silver Spring, MD, United States of America*

***Baek J.H. and D'Agnillo F. are both corresponding Author**

Arrived: 13 December 2023
Revision accepted: 12 April 2024
Correspondence: Felice D'Agnillo
e-mail: felice.dagnillo@fda.hhs.gov

Background - Quality assessment of modified or processed red blood cell (RBC) components, such as pathogen-reduced RBCs, using only *in vitro* testing may not always be predictive of *in vivo* performance. Mouse or rat *in vivo* models are limited by a lack of applicability to certain aspects of human RBC biology. Here, we used a guinea pig model to study the effects of riboflavin combined with UV light on the integrity of RBCs *in vitro* and following transfusion *in vivo*.
Materials and methods - Guinea pig RBCs were collected from whole blood (WB) treated with varying UV doses (10, 20, 40 or 80 J/mL) in the presence of riboflavin (UVR-RBCs). *In vitro* tests for UVR-RBCs included hemolysis, osmotic fragility, and cellular morphology by scanning electron microscopy. Guinea pigs transfused with one-day post-treatment UVR-RBCs were evaluated for plasma hemoglobin (Hb), non-transferrin bound iron (NTBI), total iron and Perls-detectable hemosiderin deposition in the spleen and kidney, and renal uptake of Hb.
Results - Acute RBC injury was dose dependently accelerated after treatment with UV light in the presence of riboflavin. Aberrant RBC morphology was evident at 20, 40, and 80 J/mL, and membrane lysis with Hb release was prominent at 80 J/mL. Guinea pigs transfused with 40 and 80 J/mL UVR-RBCs showed increased plasma Hb levels, and plasma NTBI was elevated in all UVR-RBC groups (10-80 J/mL). Total iron levels and Perls-hemosiderin staining in spleen and kidney as well as Hb uptake in renal proximal tubules were increased 8 hours post-transfusion with 40 and 80 J/mL UVR-RBCs.
Discussion - UVR-RBCs administered to guinea pigs increased markers of intravascular and extravascular hemolysis in a UV dose-dependent manner. This model may allow for the discrimination of RBC injury during testing of extensively processed RBCs intended for transfusion.

Keywords: *blood safety, pathogen reduction, red blood cells, animal models.*

INTRODUCTION

Appropriate preclinical testing of modified blood components is essential to support early phase development of technologies used to improve the safety and availability of blood and blood components. For example, pathogen reduction technologies (PRTs)

Blood Transfus 2024; 22: 316-327 doi: 10.2450/BloodTransfus.718

can be used to reduce the risk of transfusion transmitted infections (TTIs) and accelerate the response to novel or emerging infectious threats[1-6]. PRTs may also be used to inactivate residual white blood cells in donor blood, which helps reduce the threat of life-threatening immune-mediated complications such as transfusion-associated graft-versus-host disease. However, PRTs, which to date have mostly targeted pathogens through the physicochemical disruption of structural elements or the modification of nucleic acids to prevent replication, can have off-target effects[6-11]. In addition, the absorption of light by hemoglobin (Hb) inside RBCs, at wavelengths in the UV region and most of the visible spectrum, is a major technical hurdle that has limited illumination based approaches for RBCs and whole blood (WB)[10,11]. WB PRTs are also difficult to optimize because different blood components may react differently to the treatment, which can adversely affect the quality and viability of the individual PRT-derived products or lead to inadequate inactivation of pathogens[7,12,13]. Several studies have examined WB treatment with the non-light activated Intercept Blood System for RBCs (S-303/glutathione) and the Mirasol system (UV light/riboflavin)[11,14-17]. Progress in this field has encouraged further efforts to identify safe, effective, and broadly applicable WB PRTs that could have important practical and economic implications for the blood supply, including potentially reducing or eliminating certain donor deferral and/or testing requirements[3,11].

Although such technologies are promising, to accelerate their development and translation to clinical studies, preclinical models that can potentially predict clinical safety and effectiveness, and which typically require significant investment, remain an area of need. *In vitro* quality tests for pathogen-reduced RBCs are used to determine the structural and functional integrity of RBCs immediately after PRT treatment or during storage, however, these *in vitro* methods alone are not fully predictive of RBC safety or function post-transfusion[18,19]. In this regard, useful information may be gleaned from studying physiologically relevant and inexpensive small animal transfusion models that may help further define the predictive and correlative value of *in vitro* RBC tests. Commonly used rodent models (e.g., mouse and rat) are limited by a lack of comparability to certain aspects of human RBC physiology such as size, deformability, and oxidative biology, even when Hb concentrations and hematocrit are similar[20,21]. Previous studies have established the guinea pig as a useful small animal species to model transfusion processes and human RBCs[21-26]. Guinea pigs, unlike other rodents, are unable to synthesize ascorbate *de novo* and, like some non-human primates and humans, rely on dietary intake and glutathione-dependent recycling to cope with oxidant stress. This is highly relevant in RBC physiology, particularly when modeling blood storage that can exacerbate RBC damage[21].

In the present study, we used a guinea pig model to study the effects of riboflavin combined with UV light, as a potential mode of WB or RBC treatment, on the integrity of RBCs *in vitro* and following transfusion *in vivo*. First, we collected guinea pig RBCs from WB treated with riboflavin and increasing doses of UV light (UVR-RBCs). Second, we evaluated the UV dose-dependent changes on *in vitro* hemolysis, osmotic fragility, and RBC morphology. Then, guinea pigs were transfused with one-day stored UVR-RBCs to comparatively assess the impact of different UV doses on plasma Hb, non-transferrin bound iron (NTBI), tissue iron, and Hb deposition. The present findings suggest this guinea pig transfusion model may be useful for detecting early adverse changes to UVR-RBCs that increase their vulnerability to intravascular and extravascular hemolytic processes.

MATERIALS AND METHODS

Animal surgery and WB collection

Male Hartley guinea pigs were purchased from Charles Rivers Laboratories (Wilmington, MA, USA) and acclimated for 2-3 weeks. All animals were fed normal diets and weighed 400-600 g at the time of study. Thirty guinea pigs were used as WB donors. Surgical placement of carotid artery catheter was performed as previously described[24]. WB was drawn aseptically under anesthesia via the carotid artery catheter into 20 mL syringes containing 15% Anticoagulant Citrate Phosphate Double Dextrose (CP2D) (Pall Corporation, Port Washington, NY, USA). Collections were pooled (6 donors per pool, 100-120 mL blood) and leukocyte-reduced using a neonatal high efficiency leukocyte reduction filter and storage bag, designed to hold 175 mL volumes and approximate the plasticizer composition of standard units that incorporate polyvinylchloride (PVC) and the phthalate plasticizer

di(2-ethylhexyl phthalate) (Purecell Neo, Pall Corporation). Blood bags were kept at 4-6°C until treatment with UV light on the same day of WB collection.

UV light treatment

A UV lamp emitting rays between 280 nm and 360 nm (peak ~305-310 nm) was obtained from Fisher Scientific (Hampton, NH, USA). Fresh riboflavin (50 mM) was prepared in 0.9% NaCl (Sigma, St. Louis, MO, USA). Guinea pig WB (43 to 66 mL) was mixed with riboflavin (final concentration 50 μM) in a Terumo BCT blood bag (Lakewood, CO, USA) and placed on a GyroTwister 3-D laboratory shaker (Labnet, Edison, NJ, USA) at a speed of 50 rpm/min during UV exposure at room temperature (RT). The UV dose delivered over a given time was determined using a radiometer (Model UVX-36, UVP, Upland, CA, USA). The total UV dose was calculated as units of J/mL of WB. After UV treatment (10, 20, 40, or 80 J/mL), blood was centrifuged at 2,500 × *g* for 10 minutes and platelet poor plasma was removed. RBCs were then supplemented with additive solution formula 3 (AS-3, Pall Corporation), with each 100 mL containing Dextrose Monohydrate 1.10 g; Trisodium Citrate Dihydrate 0.59 g; Sodium Chloride 0.41 g; Monobasic Sodium Phosphate Monohydrate 0.28 g; Citric Acid Monohydrate 0.042 g; Adenine 0.03 g; and Water for Injection, to give a hematocrit of 60-70% (3 separate RBC storage bags). AS-3 was previously shown to be an effective storage solution for guinea pig RBCs[21]. UVR-RBCs were stored for one day at 4-6°C prior to transfusion experiments.

Hemolysis and osmotic fragility analyses

Cell-free Hb present in untreated or UVR-treated WB supernatants was measured spectrophotometrically at 414 nm after centrifugation at 1,000 × *g* for 10 minutes at RT (Agilent 8453 Spectrophotometer, Agilent Technologies, Rockville, MD, USA). Absorbance readings were compared to a series of diluted hemolyzed blood standard. The value was finally normalized by % of hemolysis of total hematocrit as follows: *(100-hematocrit) × supernatant Hb/ total Hb*. For osmotic fragility, 30 μL of WB were added to tubes containing 2 mL of 0.9, 0.6, 0.5, 0.4, 0.3, or 0% NaCl solutions. After invert mixing and incubation at RT for 20 minutes, the samples were centrifuged, and the supernatants were analyzed for hemolysis as described above.

RBC morphology by scanning electron microscopy

UVR-RBCs on the same-day of treatment or after one-day storage at 4°C were fixed (1% glutaraldehyde in 0.1 M phosphate buffer) and post-fixed with 1% osmium tetroxide for 1 hour at RT as previously described[24]. Samples were viewed using a TESCAN Mira3 FE-Scanning Electron Microscope. Images were acquired using a TESCAN digital camera and analyzed for the presence of RBCs characterized as echinocytes/acanthocytes (irregular spicules/regular spicules), stomatocytes (cup- or bowl-shaped), and kinzocytes (two concavities). The % altered morphology score was calculated by dividing the total number of RBCs with any of these morphological alterations by the total number of RBCs present in each image (3-4 images per sample). The mean % altered morphology values ± SEM were derived for each treatment group.

Exchange transfusion procedure

Guinea pigs were allocated to five separate transfusion groups: 50% exchange transfusion with untreated blood or UVR-RBCs prepared at doses of 10, 20, 40, or 80 J/mL (5 animals for each group). Prior to transfusion, UVR-RBCs were diluted to 45% hematocrit with normal guinea pig plasma. Exchange transfusion was carried out in conscious and freely moving animals at a rate of 1 mL/min using carotid and jugular catheters (50% ~12-18 mL blood replaced). Blood samples (350 μL) were collected prior to transfusion, at the end of transfusion (0), and 1, 2, 4, and 8 hours post-transfusion. At the 8-hour time point, animals were euthanized by intraperitoneal injection of Euthasol® (Virbac, Westlake, TX, USA) femoral veins were cut, and cold saline was perfused via the arterial catheter to remove blood. Spleens and kidneys were dissected, and frozen at −80°C or fixed in 10% formalin for 24 hours before further processing.

Plasma cell-free Hb measurement

Plasma was separated from collected blood samples by centrifugation at 2,000 rpm for 10 minutes and plasma Hb concentrations were measured using the NanoDrop 2000c spectrophotometer (Thermo Scientific, Waltham, MA, USA) and calculated using multi-component analysis[26].

Plasma NTBI and tissue iron measurements

Direct measurement of plasma NTBI was performed based on the chromogenic reaction with Ferrozine (Hach, Loveland, Colorado, USA) with spectrophotometric detection at 562 nm using a BioTek Synergy microplate

reader (Agilent Technologies), as previously described[25]. Direct iron measurement of spleen and kidney tissue (100 mg) was based on the chromogenic reaction of processed homogenates with Ferrozine in the presence of ascorbic acid for 30 minutes followed by spectrophotometric detection at 560 nm, as previously described[24].

Histochemical detection of tissue hemosiderin iron

Spleen and kidney ferric iron deposition primarily associated with hemosiderin was detected using the Perls method with 5% potassium ferrocyanide and diaminobenzidine intensification as previously reported[26].

Immunofluorescence analyses

Formalin-fixed paraffin-embedded kidney sections 3 µm thick were processed, stained, and imaged as previously described[27]. Primary antibodies for Hb alpha subunit (ab82871) and aquaporin-1 (ab168387) were obtained from Abcam (Waltham, MA, USA). For semiquantitative analysis of proximal tubular Hb deposition, a total of 10 randomly selected 1 mm^2 regions per renal section of the cortex were captured using the NDP.view2 analysis software (Hamamatsu Photonics, Bridgewater, NJ, USA). The number of individual Hb-positive proximal tubular segments in each 1 mm^2 region were counted, the average for each section was calculated, and the means ± SEM were derived for each treatment group (4-6 animals per treatment group).

Statistical analyses

A one-way ANOVA with a multiple comparisons test and Tukey's correction for comparisons between exchange transfusion with untreated controls and UVR-RBCs were performed. A Kruskal-Wallis test with Dunn's test for multiple comparisons was used to evaluate *in vitro* hemolysis results. Area under the curve for plasma concentration *vs* time data was calculated using the linear trapezoidal rule. Study data are presented as means ± SEM (unless indicated otherwise), and with group means and 95% confidence intervals with significance levels set at $p<0.05$. All statistical analyses were performed using GraphPad Prism, version 8 (GraphPad Inc., San Diego, CA, USA).

RESULTS

In vitro hemolysis, osmotic fragility, and morphology of UVR-RBCs

RBC hemolysis and osmotic fragility are common indicators of cellular integrity and quality. To assess the impact of UVR on guinea pig RBCs, we measured hemolysis and osmotic fragility produced at varying UV doses (10, 20, 40 or 80 J/mL) (**Figure 1A** and **B**). Hemolysis was below detection limits at 10 and 20 J/mL, elevated but not statistically significant at 40 (0.57±0.10%, p=0.08), and significantly increased at 80 J/mL (2.02±0.62%, p<0.0001) (**Figure 1A**). Negligible changes in RBC osmotic fragility were observed with all the UV doses (**Figure 1B**).

The effect of UVR on RBC morphology was assessed using scanning electron microscopy. Images were captured for UVR-RBCs immediately post-treatment and after one-day storage at 4°C (**Figure 2A** and **B**). Untreated

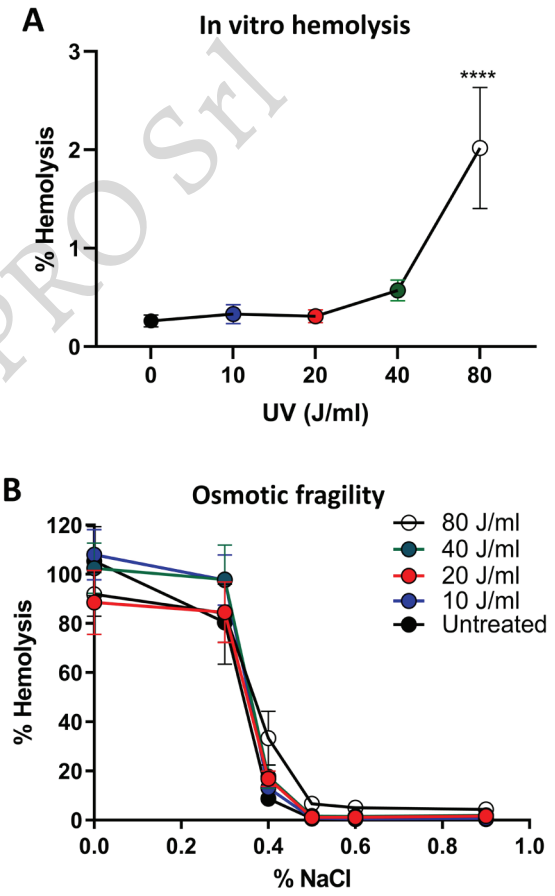

Figure 1 - *In vitro* hemolysis and osmotic fragility of UVR-RBCs. Leukocyte reduced guinea pig WB was treated with UV/riboflavin under the indicated conditions

(**A**) The percent of hemolysis in WB supernatants was measured at 414 nm, and (**B**) the osmotic fragility at varying salt conditions was assessed by measuring % hemolysis of each group (9 samples per group for untreated, 10, 40, and 80 J/mL; 6 samples for the 20 J/mL group). The differences between UVR-RBCs and untreated controls were analyzed using a one-way ANOVA. The mean values for % hemolysis ± SD for each group are shown. ****p≤0.0001 *vs* untreated controls.

RBCs showed normal discocyte morphology (**Figure 2A** and **B**). Treatment with UVR increased the number of RBCs with altered morphologies defined as echinocytes/acanthocytes (irregular spicules/regular spicules), stomatocytes (cup- or bowel-shaped) and kinzocytes (two concavities). Semiquantitative image analyses of UVR-RBCs immediately after treatment revealed significant increases in the number of RBCs with altered morphology at 40 (54.7±13.1%, p<0.0001) and 80 J/mL (43.1±6.9%, p<0.0001) (**Figure 2A**). After one-day storage, RBCs with altered morphologies were detectable at 10 J/mL (17.0±6.5%, p=0.37), and were significantly increased at 20 (24.1±8.9%, p=0.02), 40 (26.8±9.3%, p=0.004), and 80 J/mL (42.3±9.1%, p<0.0001) compared to untreated controls (8.4±2.1%) (**Figure 2B**). These results show that WB treatment with the 80 J/mL UV dose

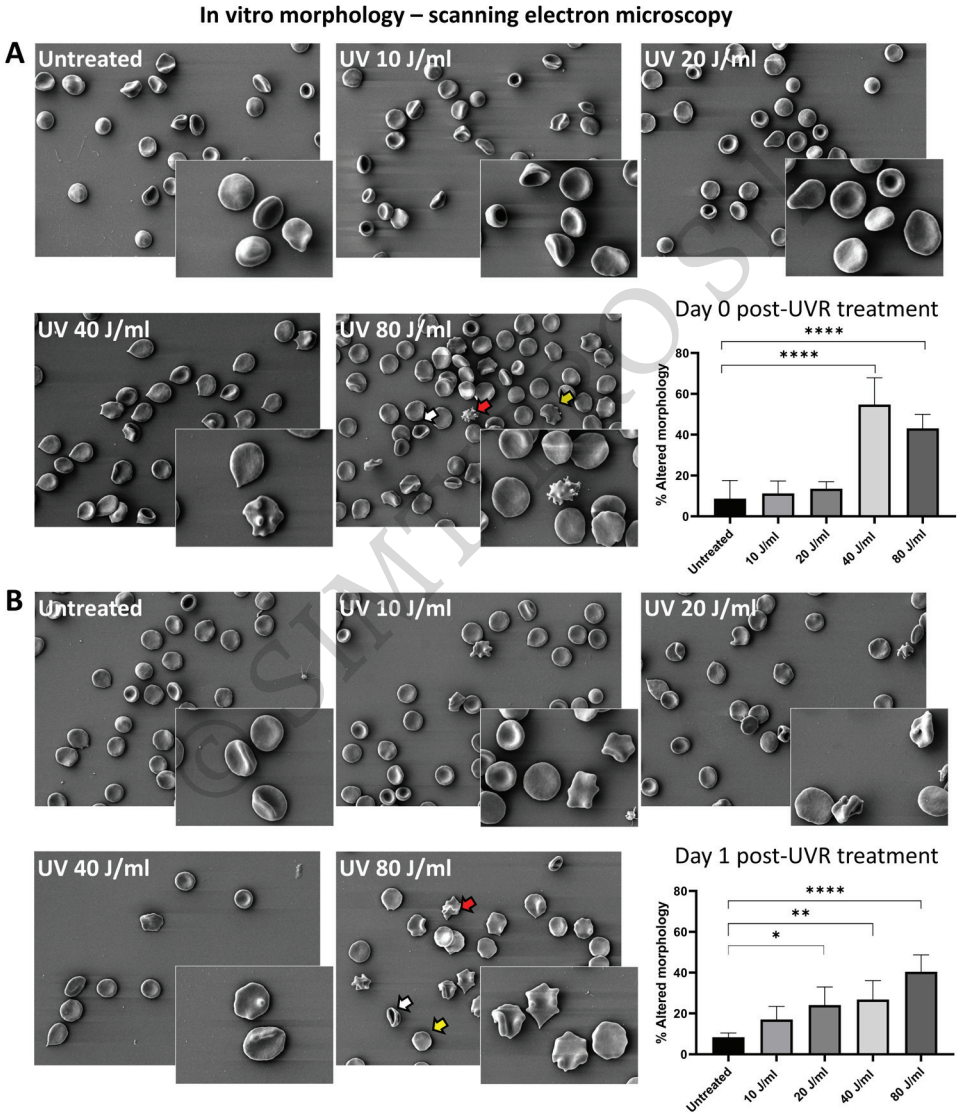

Figure 2 - Scanning electron microscopy of guinea pig UVR-RBCs
(**A**, **B**) Image analysis of UVR-RBCs just after UV treatment and after one-day storage at 4°C. Types of abnormal morphologies detected include echinocytes/acanthocytes (white arrows), stomatocytes (yellow arrows) and kinzocytes (red arrows). Bar graphs show quantitative assessment of RBCs with altered morphology (non-discoid shaped). Images were captured for each treatment group (4-6 samples per group), and the number of RBCs with altered morphology were counted and divided by the total number of RBCs. The mean % altered morphology values ± SD for each group are shown. *p≤0.05; **p≤0.01; ****p≤0.0001.

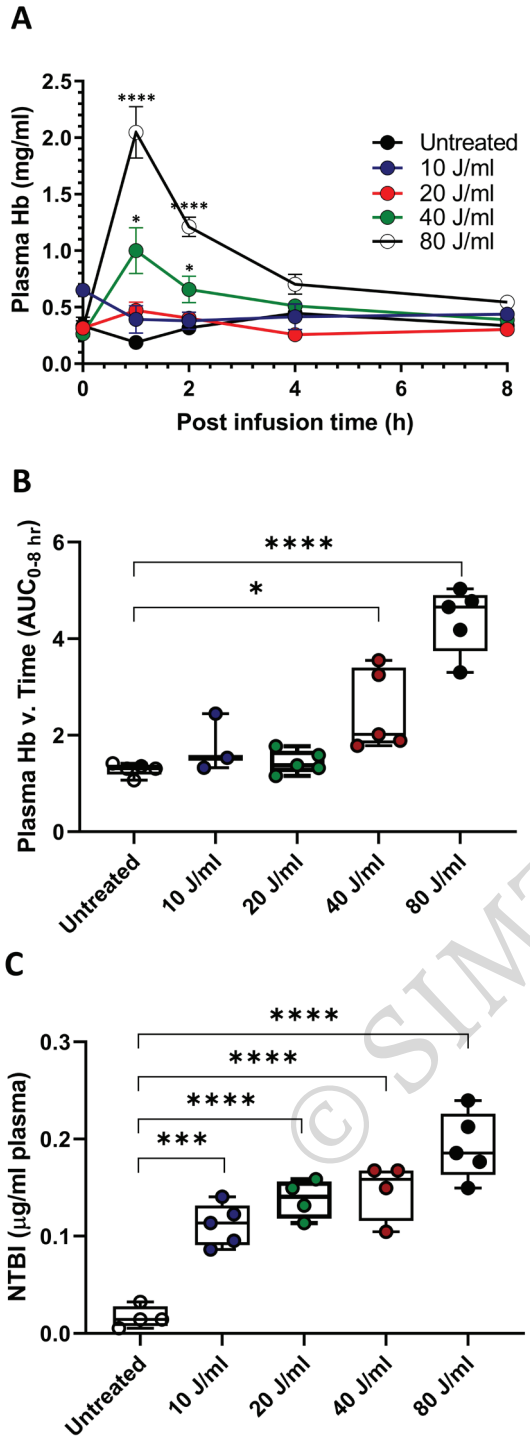

Figure 3 - Plasma Hb and NTBI levels in guinea pigs transfused with untreated RBCs or UVR-RBCs (10, 20, 40 and 80 J/mL)
(**A**) Mean plasma Hb concentration time curves were measured over the course of 8 hours post-infusion. (**B**) Individual plasma Hb values and 95% CI intervals for AUCs were calculated by the linear trapezoidal from 0-8 hours. (**C**) Plasma NTBI concentrations were measured at 8 hours post transfusion. *p≤0.05; ***p≤0.001; ****p≤0.0001 *vs* untreated controls.

produced significant levels of hemolysis, while UV doses at 20 and 40 J/mL did not result in statistically significant hemolysis but still generated morphological alterations among a significant fraction of RBCs, possibly indicating an increased vulnerability of these cells to further stress and damage.

Plasma Hb and NTBI following UVR-RBC transfusion in guinea pigs

Guinea pigs transfused with 40 and 80 J/mL UVR-RBCs showed significant increases in plasma Hb levels as early as one hour post-infusion (1.00±0.20 mg/mL, p=0.01 and 2.05±0.23 mg/mL, p<0.0001, respectively, *vs* untreated controls, 0.19±0.04 mg/mL) (**Figure 3A**). Maximum plasma concentration (Cmax) values occurred at 1 hour (Tmax) post-infusion in both groups. Similarly, areas under the plasma Hb concentration *vs* time curves from the end of transfusion until 8 hours ($AUC_{0\text{-}8hr}$) were greater after transfusion with 40 and 80 J/mL UVR-RBCs (2.45±0.37 mg/mL, p=0.023; 4.39±0.30 mg/mL, p<0.0001, respectively, *vs* untreated controls, 1.29±0.06 mg/mL) (**Figure 3B**). No significant increases in plasma Hb were observed with 10 and 20 J/mL UVR-RBCs based on Cmax and $AUC_{0\text{-}8\ hr}$ exposure. Notably, for all the transfusion groups, plasma Hb levels were similar immediately after completion of transfusion (T=0), suggesting that the levels of free Hb content present in the different UVR-RBC preparations prior to transfusion were comparable. Additional analyses revealed significant increases in plasma NTBI levels at 8 hours post-transfusion in the 10 (0.112±0.010 µg/mL, p<0.001), 20 (0.138±0.010 µg/mL, p<0.0001), 40 (0.147±0.015 µg/mL, p<0.0001), and 80 J/mL (0.193±0.015 µg/mL, p<0.0001) groups (*vs* untreated controls, 0.017±0.006 µg/mL) (**Figure 3C**).

Tissue iron deposition following UVR-RBC transfusion in guinea pigs

Non-heme iron accumulation primarily in the form of hemosiderin was visualized in the spleen and kidney using the Perls staining method at 8-hr post-transfusion[26] (**Figures 4** and **5**). In the spleen, non-heme iron was detected in the 20, 40, and 80 J/mL UVR-RBC groups (**Figure 4A**). High magnification images showed intense non-heme iron in the red pulp accompanied by decreased white pulp reactivity in these UVR-RBC groups (**Figure**

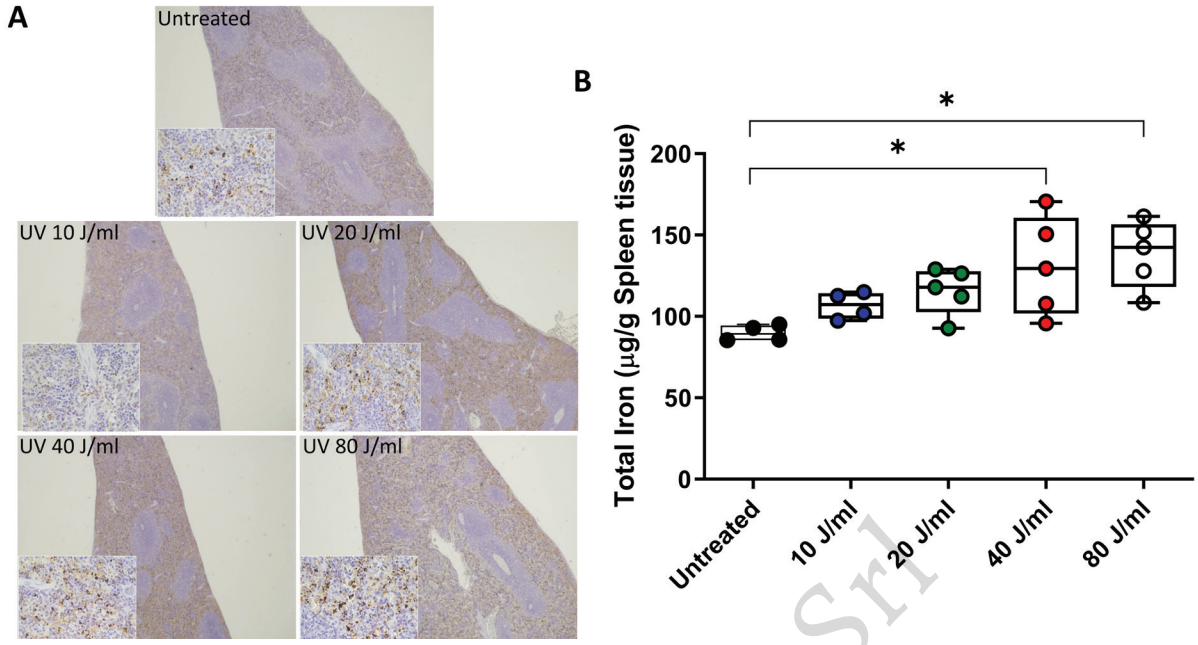

Figure 4 - Spleen hemosiderin iron deposition
(**A**) Representative Perls iron staining (brown) of guinea pig spleen 8-hours post-transfusion with untreated RBCs or UVR-RBCs at 10, 20, 40 and 80 J/mL. Total magnification 200x (inserts 600x). (**B**) Spleen total iron concentrations and 95% CI intervals at 8-hours post transfusion. *p≤0.05.

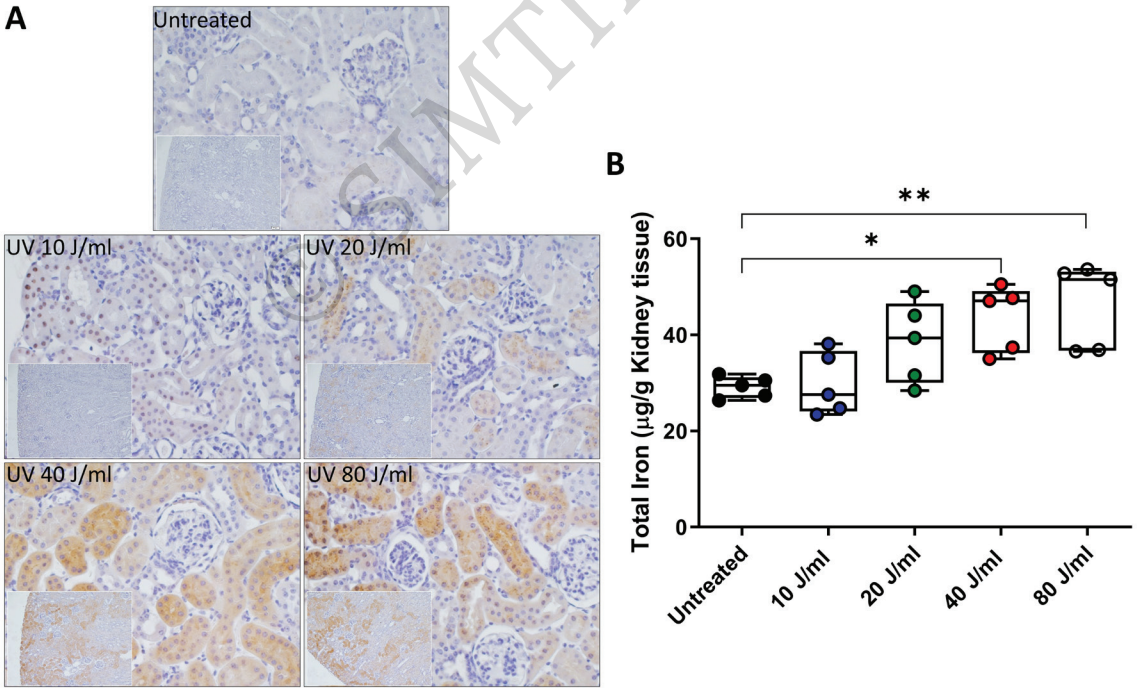

Figure 5 - Kidney hemosiderin iron deposition
(**A**) Representative Perls iron staining (brown) of guinea pig kidney 8-hours post-transfusion with untreated RBCs or UVR-RBCs at 10, 20, 40 and 80 J/mL. Total magnification 40x (inserts 600x). (**B**) Kidney total iron concentrations and 95% CI intervals at 8-hours post transfusion. *p≤0.05; **p≤0.01.

4A, *inserts*). Total splenic iron levels measured using a ferrozine-based assay revealed significant increases in the 40 and 80 J/mL UVR-RBC groups (130.8±13.7 µg/g tissue, p=0.035 and 138.4±9.3 µg/g tissue, p=0.010, respectively, *vs* untreated controls, 89.8±2.4 µg/g tissue) (**Figure 4B**). In the kidney, Perls non-heme iron was observed following transfusion with the 20, 40 and 80 J/mL UVR-RBCs (**Figure5A**). Non-heme iron accumulated mainly in the cortex with particularly intense reactivity detected in the 40 and 80 J/mL groups. Non-heme iron was not observed following transfusion with untreated RBCs or 10 J/mL UVR-RBCs. Total iron levels in the kidney were also significantly increased following transfusion of 40 and 80 J/mL UVR-RBCs (43.5±3.1 µg/g tissue, p=0.027 and 46.3±3.9 µg/g tissue,

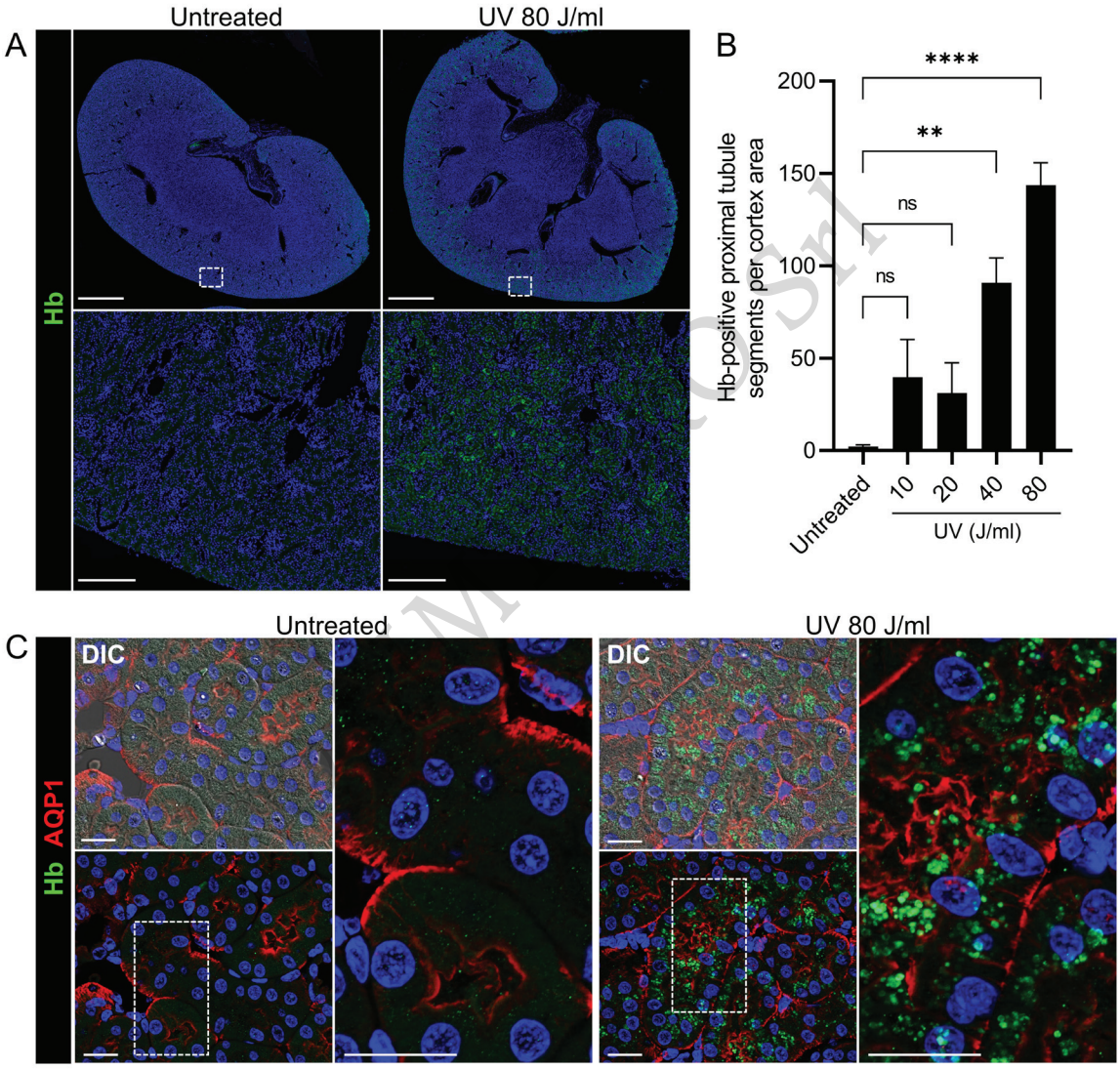

Figure 6 - Renal Hb accumulation
(**A**) Representative immunofluorescence staining for Hb in kidney sections from guinea pigs 8-hours post-transfusion with untreated RBCs or 80 J/mL UVR-RBCs. White boxed areas depict magnified areas of the renal cortex. Nuclei were counterstained with Hoechst 33342 (blue). Scale bars = 2,500 µm (low mag.), 250 µm (high mag.). (**B**) Semiquantitative image analysis of Hb-positive tubular segments. For each renal section, the number of proximal tubular segments positive for Hb deposits were counted in 10 randomly selected 1 mm^2-sized cortical regions. The mean values per individual section were calculated, and the means ± SEM for each treatment group are shown. **p≤0.005; ****p≤0.001; ns: no statistical significance. (**C**) Representative dual immunofluorescence images of Hb (green) and proximal tubule-expressed AQP-1 (red) combined with differential interference contrast. Magnified white boxed areas highlight the accumulation of endocytosed Hb in renal proximal tubular segments in animals infused with 80 J/mL UVR-RBCs but not with untreated RBCs. Scale bars = 20 µm.

p=0.007, respectively, *vs* untreated controls, 29.1±1.0 μg/g tissue) (**Figure 5B**).

Hb accumulation in guinea pig kidney

To further examine whether the observed renal iron sequestration correlates with an increase in the renal handling of cell-free Hb, kidney sections were immunostained with an antibody directed against the Hb alpha globin chain. Representative images show intense Hb immunoreactivity in the renal cortex 8-hours post-transfusion in the 80 J/mL UVR-RBC group compared to the absence of Hb staining in untreated controls (**Figure 6A**). Semiquantitative image analyses revealed low but nonsignificant cortical Hb staining in the 10 (p=0.27) and 20 J/mL (p=0.47) groups, while there was significant Hb accumulation in the 40 and 80 J/mL groups (91±13 positive tubules/area, p=0.022 and 152±11 positive tubules/area, p<0.0001, respectively, *vs* untreated controls, 2±1 positive tubules/area) (**Figure 6B**). Dual staining for Hb and AQP-1, a marker of proximal tubular epithelium, identified endocytosed Hb deposits concentrated along the apical aspects of proximal tubular segments (**Figure 6C**). This subcellular staining pattern reflects the uptake of Hb molecules from the tubular lumen consistent with the increased renal filtration of free Hb following the intravascular hemolysis of UVR-RBCs.

DISCUSSION

The present study evaluated RBCs derived from WB treated with UV light and riboflavin to assess UV-dose dependent effects on *in vitro* hemolysis/morphology and *in vivo* markers of intra- and extravascular hemolysis of UVR-RBCs in guinea pigs. *In vitro* analyses identified UV dose-dependent changes in RBC morphology and significant *in vitro* hemolysis at the maximum 80 J/mL dose. Transfusion of UVR-RBCs in guinea pigs revealed UV dose-dependent increases in plasma Hb and NTBI as well as tissue iron and Hb deposition at UV doses below 80 J/mL, suggesting that the guinea pig model is sensitive enough to detect early membrane-associated damage to RBCs that was not otherwise identified by *in vitro* hemolysis testing alone. Studying preclinical testing strategies for PRT-treated RBCs using cost-effective animal models combined with an understanding of their predictive value in relation to *in vitro* markers of RBC quality may provide useful insight into the benefits and limitations of novel PRTs, especially during the early stages of development.

WB treatment at 80 J/mL produced significant *in vitro* hemolysis compared to the undetectable or nonsignificant hemolysis at the lower doses of 10, 20, and 40 J/mL. Mechanisms that may underlie the observed hemolysis include UVR-driven reactive oxygen species (ROS)-dependent protein and lipid membrane damage, release of plasma membrane microvesicles from morphologically altered RBCs, and/or increased UVR-RBC susceptibility to centrifugal forces during sample processing[28,29]. While UVR generally induced minor changes in osmotic fragility, scanning electron microscopy identified a significant increase in the number of UVR-RBCs with echinocytosis-related changes at UV doses as low as 20 J/mL. These results suggest that UVR treatment induced sublytic cellular changes in a much larger population of UVR-RBCs than would otherwise be predicted by measuring *in vitro* hemolysis alone. Importantly, these morphologically abnormal UVR-RBCs are likely more vulnerable to subsequent stresses during storage or following transfusion, which could lead to enhanced intra- and extravascular hemolysis and circulatory clearance. Consistent with this idea, we noted significant increases in plasma Hb and NTBI levels in guinea pigs transfused with UVR-RBCs at doses below 80 J/mL. With the 40 and 80 J/mL UVR-RBC transfusion groups, increased plasma Hb levels measured one hour post-infusion likely reflect the significant early intravascular lysis of the most structurally vulnerable RBCs among the total population, and the decreasing plasma Hb levels over the remaining eight hours suggest that the clearance of plasma Hb outpaces the extent or rate of intravascular lysis of the remaining RBCs. Measurement of NTBI proved to be a particularly sensitive indicator of subtle UVR-RBC changes with significant increases observed in the 10 J/mL group. This accumulation of measurable amounts of plasma NTBI suggests the presence of acute iron overload conditions, which is likely the result of increased extravascular clearance of an abnormal subpopulation of transfused UVR-RBCs. Increased circulating plasma Hb and NTBI can result from both intra- and extravascular hemolysis of transfused RBCs, and the spleen is a particularly important site of extravascular hemolysis of morphologically altered RBCs[30-33]. Along these lines, splenic and renal iron

deposition as well as renal Hb uptake trended upwards at doses of 10 and 20 J/mL and were significantly elevated at 40 and 80 J/mL. A relevant aspect of this guinea pig model is that the renal handling and oxidative breakdown of circulating free Hb shares certain features with humans, given their similarities in tissue and intravascular antioxidant status[24-26]. Together, these findings suggest that this guinea pig model identified potential UVR-RBC quality differences *in vivo* that were not fully predicted by the measurement of a common *in vitro* marker of RBC quality (in this case hemolysis). To further strengthen comparative evaluations beyond hemolysis alone, it will be important to examine the correlative value of other *in vitro* markers of membrane damage, such as phosphatidylserine externalization, CD47 expression, potassium release, and deformability which can serve as key predictors of RBC quality[14,15,34,35].

Post-transfusion RBC recovery has long been established as a critical indicator of RBC quality following storage or other modification, such as PRT processing[36-38]. Currently, FDA regulatory benchmarks for RBC preparation and storage devices include (1) a maximum 1% *in vitro* hemolysis and (2) a 24-hour *in vivo* recovery of at least 75% after reinfusion of autologous chromium-51-labeled RBCs in healthy volunteers, at the limit of storage. While the recovery of radioactively labeled RBCs in healthy volunteers is considered the gold standard, the method is technically challenging, expensive, and not widely accessible[38]. Moreover, there are concerns that this approach may not fully capture aspects of RBC quality that can affect safety and efficacy of transfusions in potential clinical studies or use. Given the high cost of developing PRTs and other RBC processing devices and the incomplete understanding of the relationship between *in vitro* and *in vivo* RBC quality parameters, there exists reasonable and potentially valuable rationale to establish relevant measures of RBC quality in reliable small animal models that can then supplement and be developed as early correlates of clinical performance. In this context, markers of post-transfusion hemolysis, circulating NTBI levels, and the reversal of hypoxemia are relatively easy to measure in preclinical settings, and are also considered physiologically relevant parameters. It may also be useful from a feasibility and cost-savings perspective, especially during the testing of more extensive RBC processing methods, such as PRT, to study post-processed RBCs in small animal disease state models to identify determinants of RBC safety and/or clearance. This approach could allow for prediction of RBC performance and safety in acute or chronic clinical transfusion indications.

A safe and effective PRT for WB would ideally allow for maximal and broad-spectrum pathogen inactivation while minimizing collateral damage to individual blood components. Studies on the treatment of human WB and RBCs with the Intercept (S-303/glutathione) and Mirasol (UV/riboflavin) systems have both shown effective pathogen inactivation profiles and acceptable *in vitro* RBC quality after storage up to 42 days (Intercept) or 21 days (Mirasol)[11,14-17]. The shorter storage period for Mirasol-treated RBCs likely reflects the more damaging effects caused by UV light irradiation. Mirasol PRT is being used for the treatment of WB in developmental countries given its demonstrated ability to reduce the incidence of transfusion transmitted malaria[10,39,40]. In the United States, RBCs derived from Mirasol-treated WB have undergone clinical investigation[11,13]. In the present study, the in-house UV/riboflavin system was not intended to replicate the Mirasol system although there are some similarities. For example, both systems deliver UV light over a similar range of wavelengths (280-360 nm for in-house *vs* 280-400 nm for Mirasol), and both irradiate WB in the presence of a similar final riboflavin concentration (around 50 μM). However, notably, the determination of total UV dose exposures is calculated as Joules per mL RBCs for Mirasol compared to Joules per mL WB for the current, in-house experimental system. In addition, the experimental system, unlike the Mirasol PRT, has not been evaluated for its pathogen inactivation capabilities.

This study has certain limitations. First, the critical role of storage duration on UVR-RBCs was not assessed as transfusion experiments were performed one-day after UVR treatment. This short duration was intended to test the immediate effects of UVR treatment alone without adding storage time as a confounding variable; however, this one-day approach does not reflect clinical transfusion scenarios with longer stored RBC products and thus follow-up studies will need to consider the impact of RBC storage in this model. Second, the measurement of *in vitro* hemolysis one-day post-treatment captures the more immediate impact of UVR on RBCs but underestimates

the hemolysis that would likely occur with longer storage even at the low UV doses. Third, the extent of *in vitro* hemolysis produced by the maximum 80 J/mL dose (2%) already exceeds the hemolysis acceptance criteria for human RBC products (≤1% in the US and ≤0.8% in Europe, at the end of storage). Therefore, these UVR conditions would be considered excessive and not appropriate for a PRT, if a similar level of hemolysis was observed with human RBCs. Finally, while the present results indicate potentially useful implications for evaluating increased hemolysis by this animal model, further correlative studies will be needed to better understand the relevance to the clinical performance of PRT-treated RBCs.

CONCLUSIONS

RBCs derived from WB treated with riboflavin and increasing doses of UV light produced graded RBC damage *in vitro* as well as UV dose-dependent increases in markers of intravascular and extravascular hemolysis in transfused guinea pigs. Moreover, the guinea pig model appeared sensitive enough to detect the presence of UVR-RBCs with early membrane damage and increased vulnerability to hemolysis after transfusion. These findings support the potential utility of this small animal species for testing the quality of modified or post-processed RBCs and may help stimulate further proactive research on enhancing the predictive value of such preclinical studies.

ACKNOWLEDGEMENTS

We would like to thank Drs. Yiping Jia, Jana Sirsendu, and Abdu Alayash (CBER, FDA) for reviewing the manuscript.

FUNDING

This work was supported by the CBER Horizon Research Fund from the FDA (to FD and JHB).

ETHICAL CONSIDERATION

The study was approved by the FDA White Oak Institutional Animal Care and Use Committee with all experimental procedures performed in adherence to the National Institutes of Health guidelines on the use of experimental animals (#2018-06).

AUTHORS' CONTRIBUTIONS

JHB, PWB, and FD conceived of the concept and study design; JHB and FD wrote the first draft of the manuscript; JHB, HKHS, XZ, FX, YG, PWB, and FD collected and analyzed the data; JGV and FX provided study materials; JHB, MCW, PWB, CV, and FD edited the manuscript, and all Authors contributed to final approval of the manuscript.

The Authors declare no conflicts of interest.

REFERENCES

1. Busch MP, Bloch EM, Kleinman S. Prevention of transfusion-transmitted infections. Blood 2019; 133: 1854-1864. doi: 10.1182/blood-2018-11-833996.
2. Haass KA, Sapiano MRP, Savinkina A, Kuehnert MJ, Basavaraju SV. Transfusion-transmitted infections reported to the National Healthcare Safety Network Hemovigilance Module. Transfus Med Rev 2019; 33: 84-91. doi: 10.1016/j.tmrv.2019.01.001.
3. Marks P, Verdun N. Toward universal pathogen reduction of the blood supply (Conference Report, p. 3002). Transfusion 2019; 59: 3026-3028. doi: 10.1111/trf.15410.
4. Lozano M, Cid J, Prowse C, McCullough J, Klein HG, Aubuchon JP. Pathogen inactivation or pathogen reduction: proposal for standardization of nomenclature. Transfusion 2015; 55: 690. doi: 10.1111/trf.12996.
5. Prowse CV. Component pathogen inactivation: a critical review. Vox Sang 2013; 104: 183-199. doi: 10.1111/j.1423-0410.2012.01662.x.
6. Feys HB, Van Aelst B, Compernolle V. Biomolecular consequences of platelet pathogen inactivation methods. Transfus Med Rev 2019; 33: 29-34. doi: 10.1016/j.tmrv.2018.06.002.
7. Marschner S, Goodrich R. Pathogen reduction technology treatment of platelets, plasma and whole blood using riboflavin and UV light. Transfus Med Hemother 2011; 38: 8-18. doi: 10.1159/000324160.
8. Mundt JM, Rouse L, Van den Bossche J, Goodrich RP. Chemical and biological mechanisms of pathogen reduction technologies. Photochem Photobiol 2014; 90: 957-964. doi: 10.1111/php.12311.
9. Musso D, Richard V, Broult J, Cao-Lormeau VM. Inactivation of dengue virus in plasma with amotosalen and ultraviolet A illumination. Transfusion 2014; 54: 2924-2930. doi: 10.1111/trf.12713.
10. Drew VJ, Barro L, Seghatchian J, Burnouf T. Towards pathogen inactivation of red blood cells and whole blood targeting viral DNA/RNA: design, technologies, and future prospects for developing countries. Blood Transfus 2017; 15: 512-521. doi: 10.2450/2017.0344-16.
11. Atreya C, Glynn S, Busch M, Kleinman S, Snyder E, Rutter S, et al. Proceedings of the Food and Drug Administration public workshop on pathogen reduction technologies for blood safety 2018 (Commentary, p. 3026). Transfusion 2019; 59: 3002-3025. doi: 10.1111/trf.15344.
12. Allain JP, Goodrich R. Pathogen reduction of whole blood: utility and feasibility. Transfus Med 2017; 27 (Suppl 5): 320-326. doi: 10.1111/tme.12456.
13. Yonemura S, Doane S, Keil S, Goodrich R, Pidcoke H, Cardoso M. Improving the safety of whole blood-derived transfusion products with a riboflavin-based pathogen reduction technology. Blood Transfus 2017; 15: 357-364. doi: 10.2450/2017.0320-16.
14. Dimberg LY, Doane SK, Yonemura S, Reddy HL, Hovenga N, Gosney EJ, et al. Red blood cells derived from whole blood treated with riboflavin and UV light maintain adequate cell quality through 21 days of storage. Transfus Med Hemother 2019; 46: 240-247. doi:10.1159/000495257.
15. Cancelas JA, Slichter SJ, Rugg N, Pratt PG, Nestheide S, Corson J, et al. Red blood cells derived from whole blood treated with riboflavin and ultraviolet light maintain adequate survival in vivo after 21 days of storage. Transfusion 2017; 57: 1218-1225. doi: 10.1111/trf.14084.
16. Larsson L, Ohlsson S, Andersson TN, Watz E, Larsson S, Sandgren P, et al. Pathogen reduced red blood cells as an alternative to irradiated and washed components with potential for up to 42 days storage. Blood Transfus 2024; 22: 130-139. doi: 10.2450/BloodTransfus.479.

17. Brixner V, Kiessling AH, Madlener K, Müller MM, Leibacher J, Dombos S, et al. Red blood cells treated with the amustaline (S-303) pathogen reduction system: a transfusion study in cardiac surgery. Transfusion 2018; 58: 905-916. doi: 10.1111/trf.14528.
18. Wagner SJ. Developing pathogen reduction technologies for RBC suspensions. Vox Sang 2011; 100: 112-121. doi: 10.1111/j.1423-0410.2010.01386.x.
19. Benjamin RJ, McCullough J, Mintz PD, Snyder E, Spotnitz WD, Rizzo RJ et al. Therapeutic efficacy and safety of red blood cells treated with a chemical process (S-303) for pathogen inactivation: a Phase III clinical trial in cardiac surgery patients. Transfusion 2005; 45: 1739-1749. doi: 10.1111/j.1537-2995.2005.00583.x.
20. Varga A, Matrai AA, Barath B, Deak A, Horvath L, Nemeth N. Interspecies diversity of osmotic gradient deformability of red blood cells in human and seven vertebrate animal species. Cells 2022; 11: 1351. doi: 10.3390/cells11081351.
21. Bertolone L, Shin HKH, Baek JH, Gao Y, Spitalnik SL, Buehler PW, et al. ZOOMICS: Comparative metabolomics of red blood cells from guinea pigs, humans, and non-human primates during refrigerated storage for up to 42 days. Front Physiol 2022; 13: 845347. doi: 10.3389/fphys.2022.845347.
22. Genzer SC, Huynh T, Coleman-Mccray JD, Harmon JR, Welch SR, Spengler JR. Hematology and clinical chemistry reference intervals for inbred strain 13/n guinea pigs (cavia porcellus). J Am Assoc Lab Anim Sci 2019; 58: 293-303. doi: 10.30802/AALAS-JAALAS-18-000118.
23. Baek JH, D'Agnillo F, Vallelian F, Pereira CP, Williams MC, Jia Y, et al. Hemoglobin-driven pathophysiology is an in vivo consequence of the red blood cell storage lesion that can be attenuated in guinea pigs by haptoglobin therapy. J Clin Invest 2012; 122: 1444-1458. doi: 10.1172/JCI59770.
24. Baek JH, Yalamanoglu A, Brown RP, Saylor DM, Malinauskas RA, Buehler PW. Renal toxicodynamic effects of extracellular hemoglobin after acute exposure. Toxicol Sci 2018; 166: 180-191. doi: 10.1093/toxsci/kfy193.
25. Baek JH, Yalamanoglu A, Gao Y, Guenster R, Spahn DR, Schaer DJ, et al. Iron accelerates hemoglobin oxidation increasing mortality in vascular diseased guinea pigs following transfusion of stored blood. JCI Insight 2017; 2: e93577. doi: 10.1172/jci.insight.93577.
26. Baek JH, Zhang X, Williams MC, Hicks W, Buehler PW, D'Agnillo F. Sodium nitrite potentiates renal oxidative stress and injury in hemoglobin exposed guinea pigs. Toxicology 2015; 333: 89-99. doi: 10.1016/j.tox.2015.04.007.
27. Williams MC, Zhang X, Baek JH, D'Agnillo F. Renal glomerular and tubular responses to glutaraldehyde-polymerized human hemoglobin. Front Med (Lausanne) 2023; 10: 1158359. doi: 10.3389/fmed.2023.1158359.
28. van Meer G, Voelker DR, Feigenson GW. Membrane lipids: where they are and how they behave. Nat Rev Mol Cell Biol 2008; 9: 112-124. doi: 10.1038/nrm2330.
29. Nguyen DB, Ly TB, Wesseling MC, Hittinger M, Torge A, Devitt A, et al. I. Characterization of microvesicles released from human red blood cells. Cell Physiol Biochem 2016; 38: 1085-1099. doi: 10.1159/000443059.
30. Hod EA, Brittenham GM, Billote GB, Francis RO, Ginzburg YZ, Hendrickson JE, et al. Transfusion of human volunteers with older, stored red blood cells produces extravascular hemolysis and circulating non-transferrin-bound iron. Blood 2011; 118: 6675-6682. doi: 10.1182/blood-2011-08-371849.
31. Vallelian F, Buehler PW, Schaer DJ. Hemolysis, free hemoglobin toxicity, and scavenger protein therapeutics. Blood 2022; 140: 1837-1844. doi: 10.1182/blood.2022015596.
32. Youssef LA, Rebbaa A, Pampou S, Weisberg SP, Stockwell BR, Hod EA, et al. Increased erythrophagocytosis induces ferroptosis in red pulp macrophages in a mouse model of transfusion. Blood 2018; 131: 2581-2593. doi: 10.1182/blood-2017-12-822619.
33. Roussel C, Morel A, Dussiot M, Marin M, Colard M, Fricot-Monsinjon A, et al. Rapid clearance of storage-induced microerythrocytes alters transfusion recovery. Blood 2021; 137: 2285-2298. doi: 10.1182/blood.2020008563.
34. Qadri SM, Chen D, Schubert P, Perruzza DL, Bhakta V, Devine DV, et al. Pathogen inactivation by riboflavin and ultraviolet light illumination accelerates the red blood cell storage lesion and promotes eryptosis. Transfusion 2017; 57: 661-673. doi: 10.1111/trf.13959.
35. Wagner SJ, Skripchenko A, Thompson-Montgomery D, Awatefe H. Evaluation of the sensitivity of red blood cell markers to detect photodynamic membrane damage. Transfusion 2004; 44: 716-721. doi: 10.1111/j.1537-2995.2004.03356.x.
36. Franco RS. The measurement and importance of red cell survival. Am J Hematol 2009; 84: 109-114. doi: 10.1002/ajh.21298.
37. Mock DM, Widness JA, Veng-Pedersen P, Strauss RG, Cancelas JA, Cohen RM, et al. Measurement of posttransfusion red cell survival with the biotin label. Transfus Med Rev. 2014; 28: 114-125. doi: 10.1016/j.tmrv.2014.03.003.
38. Roussel C, Buffet PA, Amireault P. Measuring post-transfusion recovery and survival of red blood cells: strengths and weaknesses of Chromium-51 labeling and alternative methods. Front Med (Lausanne) 2018; 5: 130. doi: 10.3389/fmed.2018.00130.
39. Allain JP, Owusu-Ofori AK, Assennato SM, Marschner S, Goodrich RP, Owusu-Ofori S. Effect of Plasmodium inactivation in whole blood on the incidence of blood transfusion-transmitted malaria in endemic regions: the African Investigation of the Mirasol System (AIMS) randomised controlled trial. Lancet 2016; 387: 1753-1761. doi: 10.1016/S0140-6736(16)00581-X.
40. Kasirye R, Hume HA, Bloch EM, Lubega I, Kyeyune D, Shrestha R, et al. The Mirasol Evaluation of Reduction in Infections Trial (MERIT): study protocol for a randomized controlled clinical trial. Trials 2022; 23: 257. doi: 10.1186/s13063-022-06137-8.